BED SHEAR STRESS MEASUREMENTS IN DAM BREAK AND SWASH FLOWS

Matthew P. Barnes & Tom E. Baldock
Department of Civil Engineering, The University of Queensland, Brisbane 4072, Australia

ABSTRACT

A novel shear plate was used to make direct bed shear stress measurements in laboratory dam break and swash flows on smooth, fixed, impermeable beds. The pressure gradient due to the slope of the fluid free-surface across the plate was measured using pressure transducers. Surface elevation was measured at five locations using acoustic displacement sensors. Flow velocity was measured using an Acoustic-Doppler Velocimeter and calculated using the ANUGA inundation model. The measured bed shear stress at the dam break fluid tip for an initially dry, horizontal bed was close to twice that estimated using steady flow theory. The temporal variation of swash bed shear stress showed a large peak in landward directed stress at the uprush tip, followed by a rapid decay throughout the uprush flow interior. The peak seaward directed stress during the backwash phase was less than half that measured in the uprush. Close to the still water line, in the region of bore collapse and at the time of initial uprush, favourable pressure gradients were measured. In the lower swash region predominately weak adverse pressure gradients were measured.
Keywords: bed shear stress, swash, dam break, pressure gradient.

INTRODUCTION

For mobile bed environments knowledge of the boundary shear stress, the force imparted on the bed by the fluid flowing over it, is of particular importance to sediment transport modelling. Obtaining accurate measurements or estimates of boundary shear stress in unsteady flow remains a challenge. Difficulties are commonly associated with the design of suitable instrumentation for measuring fluctuating flow characteristics. In the case of nearshore coastal environments, the interaction of tidal and wave currents produces turbulent boundary layer velocities and instantaneous bed friction force vectors that fluctuate both in magnitude and direction. Even greater hydraulic complexity is encountered within the swash zone, the region of beach intermittently exposed to the atmosphere due to fluid uprushes and backwashes. Additional processes that may influence swash zone sediment transport include bore induced turbulence (Jackson *et al*., 2004; Pritchard and Hogg, 2005), rapid boundary layer growth (Masselink *et al*., 2005), and the effects of infiltration-exfiltration (e.g. Butt *et al*., 2001).

Sediment transport modelling typically relies on bed shear stress estimates indirectly derived from the near bed logarithmic velocity profile or the quadratic drag law. Close to the

bed boundary, the current velocity U varies with the height z above the bed according to the logarithmic velocity profile

$$U(z) = \frac{u_*}{\kappa} \ln\left(\frac{z}{z_0}\right) + D_1 \tag{1}$$

where u_* is the friction velocity, z_0 is the bed roughness length, and κ is von Karman's constant ($\kappa \approx 0.41$). Schlichting (1979) defines the constant D_1 as $5.5U$ for smooth turbulent flow and $8.5U$ for fully rough turbulent flow. Equation 1 is commonly referred to as the law-of-the-wall or the log law. The friction velocity u_* is related to the bed shear stress τ_0 through the relationship $\tau_0 = \rho u_*^2$ where ρ is the fluid density. The bed shear stress is commonly related to the depth-averaged fluid velocity $\overline{U}$ through the friction coefficient C_f

$$\tau_0 = C_f \frac{1}{2} \rho \overline{U}^2 \tag{2}$$

C_f is related to the widely applied Darcy friction factor f through

$$f = 4C_f \tag{3}$$

Equation 2 has been shown to successfully predict bed shear stress for steady flow conditions. The applicability of Eq. 2 in unsteady flow remains uncertain, although universally applied in wave loading and bed shear stress calculations.

In the swash zone the backwash is not simply the opposite of the uprush. Sediment transport modelling in the swash zone that considers transport to be a simple function of velocity (Energetics models) typically result in predictions of net offshore transport due to uprush/backwash asymmetry (e.g. Masselink and Hughes, 1998). The stability of most beaches implies that other processes not accounted for by a simple Energetics approach must contribute to onshore directed sediment transport.

The investigation of the vertical structure of swash flows and bed shear stress is limited to a few experimental and field studies. Laboratory investigations by Cox *et al*. (2000) and Cowen *et al*. (2003) reported estimates of shear stress in the inner surf and swash zone with an impermeable bed by fitting mean velocity profile data to the log law. Both Cox *et al*. (2000) and Cowen *et al*. (2003) found the uprush C_f to be typically greater than the backwash C_f however the magnitude of C_f varied between the two studies. Field estimates of bed shear stress and C_f at the uprush tip by Hughes (1995) and later Puleo and Holland (2001) differed by order of magnitude. The discrepancies in the description of bed shear stress and estimates of C_f in laboratory and field swash may be attributed to differences between friction at the landward swash edge and in the flow interior, or to the breakdown of logarithmic layer and model assumptions (Raubenhiemer *et al.* 2004).

Direct measurements of bed shear stress in experimental open channels or wave flumes are generally restricted to devices that measure the integrated force on a flush mounted shear plate (e.g. Riedel and Kamphuis, 1973; Grass *et al*. 1995) or thermal techniques such as hot film anemometry (e.g. Gust and Southard, 1983; Paola *et al*. 1986). Some success has been reported with hot film bed shear stress measurements in field swash (Conley and Griffin, 2004) however the technique is traditionally limited by calibration difficulties and/or obtaining a relationship between heat transfer and bed shear stress.

The present investigation has been prompted by a need for improved knowledge in the applicability of laboratory and field studies of bed shear stress in swash flows. A shear plate with a fundamental design based on the UCL shear cell (Grass *et al*. 1995) is used to obtain direct shear stress measurements in laboratory dam break and swash flows. The dam break problem and the effect of friction is of interest here since an analogy can be drawn with the run-up of a solitary wave (Carrier *et al*. 2003) or with swash motion following bore collapse (Shen and Meyer, 1963; Peregrine and Williams, 2001; Pritchard and Hogg, 2005).

EXPERIMENTS

Experiments were conducted at The University of Queensland (UQ) Gordon McKay Hydraulics Laboratory using two facilities – a dam break flume and a solitary wave flume. In each facility a novel shear plate (Figure 1) was installed allowing direct shear stress measurement.

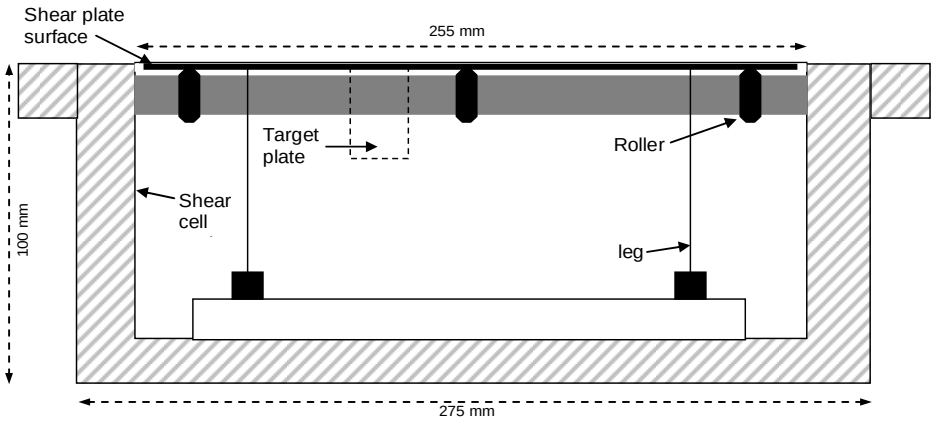

Figure 1. Shear plate cross-sectional diagram.

The aluminium shear plate is 0.1 m long, 0.25 m wide and 0.73 mm thick. Four stainless steel tubular legs are clamped to the underside of the plate and extend to the base of the shear plate's casing (referred herein as 'cell') where they are fixed. Below the plate two bars fitted with stainless steel ball bearing rollers extend longitudinally, offering support against hydrostatic loading. A positive displacement approach is adopted whereby the applied shear forces cause the plate to be displaced in the horizontal direction of the shear. To allow for the displacement, a 1mm gap exists between the longitudinal plate edge and the cell casing. Any horizontal shear applied across the plate causes the four support legs to flex in the direction of the shear, shifting the plate a distance directly proportional to the force. The horizontal displacement vector of the shear plate is measured by a single Indikon Eddy-current Proximity Probe aligned perpendicular to a target plate attached on the underside of the shear plate.

During operation the shear cell is filled with water to the level of the 1 mm gaps at the longitudinal plate edges. The pressure inside the cell is hydrostatic. The pressure gradient $\partial p/\partial x$ that may exist across the shear plate due to the slope of the free-surface is measured via two Druck PMP 317-2780 pressure transducers with ±0.15% accuracy (GE Druck, 2006). The measured pressure in the gaps at the longitudinal plate edges is a secondary force capable of producing work on the small area of the plate's edge (i.e. plate width × thickness). Subsequently, if a pressure gradient exists it will influence the plate's displacement. The significance of this additional force needs consideration when resolving the direct shear stress measurements.

Dam Break Experiments

Experiments were conducted in a tilting flume 4 m long, 0.4 m wide and 0.4 m high (Figure 2). The flume has an impermeable PVC bed (roughness height, $k_s \approx 0.1$ mm) and clear glass walls. One end of the flume is permanently closed. The other end is open to allow over-topping. A dam gate can be located at any position along the flume's length acting to hold a reservoir of desired volume. The gate is PVC, 12 mm thick, with a silicon seal at the base and sides. The seal together with a small amount of silicon grease eliminate any leakage from the reservoir. Consequently, the bed in front of the gate is completely dry. Connected to the gate is a pivoting arm that opens and closes the gate. The gate is operated manually. Video analysis indicates that the gate opens to a height > 0.2 m in approximately 0.12 s.

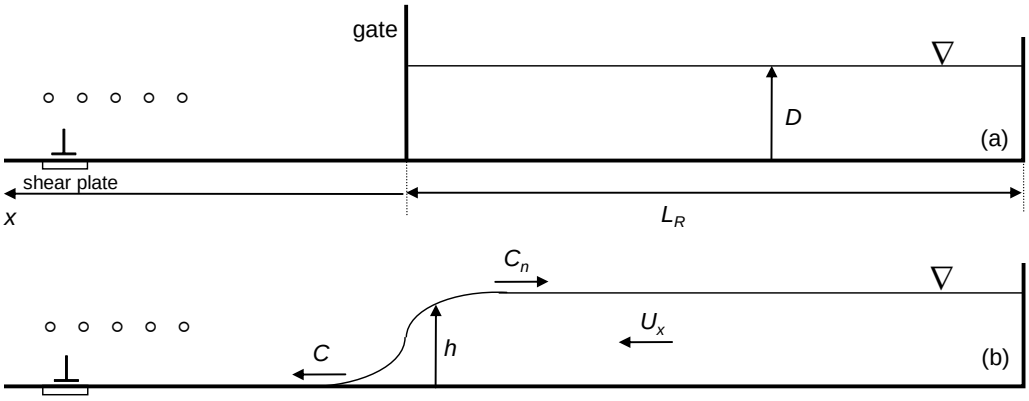

Figure 2. Dam break flume with initial reservoir depth D and length L_R (a). Dam break propagation following gate removal (b). C is surge front celerity, C_n is negative wave celerity, U_x is fluid velocity, and h is the flow depth, and ∇ is the still water line. "○" Indicates MS sensor locations; "⊥" indicates ADV location.

Direct shear stress τ_0 measurements for a propagating dam break were obtained using the shear plate installed 0.3 m (measured from the plate's centre) from the open end of the flume. Free surface elevation η was measured at five cross-flume locations (0.1 m spacing) using an array of Microsonic (MS) Mic+25/IU/TC acoustic displacement sensors with an accuracy of 0.18 mm and response time of 50 ms (Microsonic, 2005). MS sensor 4 and 5 were aligned with the leading and trailing edge of shear plate (see Fig. 2). Instantaneous velocities were recorded using a SonTek micro Acoustic Doppler Velocimeter (ADV) 16 MHz. The ADV has a two-dimensional side looking head located close to the bed with a horizontal distance to sample volume of 0.05 m. The ADV was positioned to the side and central to the shear plate so that the sample volume was above the shear plate. The U_x velocity component was aligned longitudinally to the flow direction and the U_y component orientated normal to the channel side wall.

Experiments were conducted for a range of initial dam depths D, bed slopes S_o, and gate positions. Changing the dam gate position subsequently changes the distance of dam break propagation before reaching the fixed measurement location.

Wave Flume Experiments

Solitary wave (bore) experiments were conducted in a wave flume 0.85 m wide, 0.75 m high, with a bore propagation distance of approximately 8 m (Figure 3). The flume has an impermeable bed, glass walls, and 1:10 beach slope constructed from smooth, painted marine plywood. A single bore is generated by a piston wave maker with bore height H controlled by

the piston stroke length L and speed V. Provided the piston stroke is of sufficient speed (controlled by a falling weight) the bore generates at the wave maker paddle and is assumed fully developed upon reaching the shoreline.

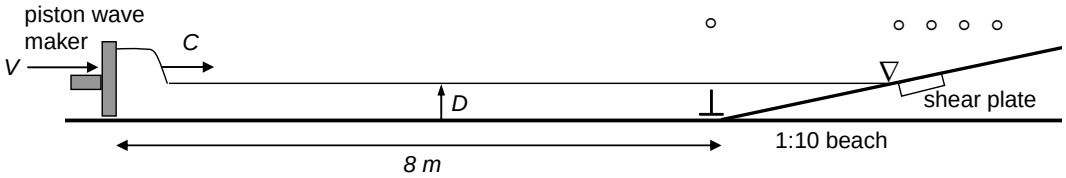

Figure 3. Wave Flume with initial depth D. C is bore celerity, and ∇ is the still water line, "∘" Indicates MS sensor locations; "⊥" indicates ADV location.

Direct shear stress τ_0 measurements at laboratory swash cycle were obtained using the shear plate installed in the beach. Free surface elevation η was measured at four cross-shore locations (0.1 m spacing) using an array of MS sensors. Instantaneous free-stream velocity components U_x and U_y were measured using an ADV located at the beach toe. A single MS sensor was aligned above the ADV sample volume to measure bore H.

Experiments were conducted for a range of initial depth D and distances to the fixed measurement location relative to the still-water line (SWL). Consequently, the variation of shear stress with time was investigated at various positions within the laboratory swash zone.

Data Acquisition and Processing

Data acquisition and instrument synchronisation was performed using LabView v7.1 and Horizon ADV v.1.04. ADV external synchronisation error is expected to be < 1 ms (Sontek, 2001). Velocity data was post-processed using WinADV v2.010. Velocity samples with a signal correlation coefficient < 70 % or a signal-to-noise ratio < 15 dB were disregarded.

RESULTS

Dam Break Experiments

The typical temporal variation of h, τ_0, and U_x for a horizontal dry bed with initial reservoir depth D = 0.2 m is shown in Figure 4. Time t = 0 is when the dam gate is opened. Reservoir length L_R = 2.25 m and the shear plate centre is at x = 0.45 m. Depth h obtained using a MS sensor above the leading edge of the shear plate clearly indicates the region at the wave tip where the effects of resistance are important (e.g. Dressler, 1954). The maximum shear stress τ_0 is measured at the wave tip followed by a rapid decay to a quasi-constant τ_0 value for t > 4 s. Fig. 4c highlights the difficulties in obtaining velocity measurements at the tip of a dam break wave (analogous to a swash uprush). Reliable U_x samples were only obtained for approximately t > 6 s. Complications are associated with the intrusive nature of the ADV probe, the response time of the instrument (once suddenly engulfed by the fluid), and shallow flow depths.

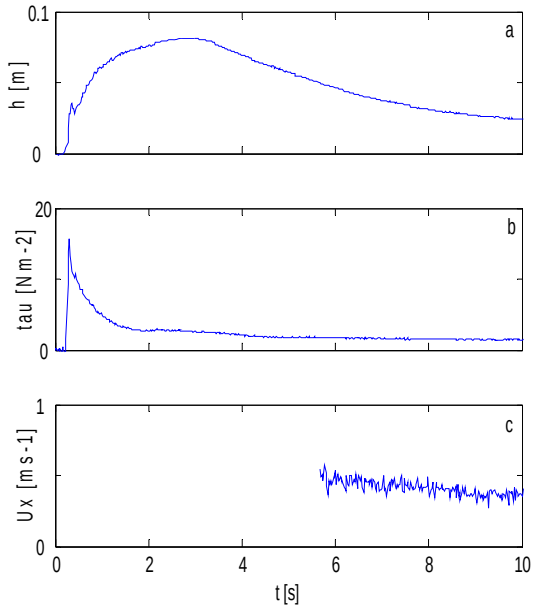

Figure 4. Typical dam break measurements on a horizontal dry bed. (a) h, (b) τ_0, and (c) U_x as a function of time.

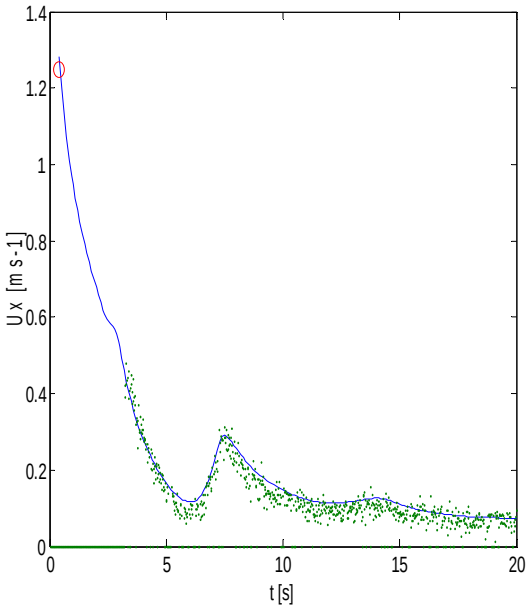

Figure 5. ANUGA model velocity (solid line) with data verification for a 1:20 bed slope and D = 0.2 m. "○" velocity obtained using MS sensors, "•" ADV samples.

U_x for t < 6 s was obtained via the ANUGA inundation model (Nielsen *et al*., 2005) modified to simulate the dam break flume. The modelled predictions were validated using the reliable ADV samples available. Figure 5 shows excellent model/data validation for a 1:20 bed slope with an initial reservoir depth D = 0.2 m. Reliable ADV samples were obtained for approximately t > 4 s. The "humps" in the velocity profile at approximately t = 2.5, 7.5, and 14 s are caused by negative waves generated by dam gate removal that propagate towards the closed end of the flume and are subsequently reflected (refer Fig. 2b). Assuming that in the region of the shallow dam break tip the flow velocity is approximately equal to the dam front celerity, a single sample for data model comparison may be obtained using the spaced MS sensors. The hollow circle at the velocity peak in Fig. 5 was obtained via the MS sensors aligned above the leading and trailing edges of the shear plate.

Figure 6a shows measured shear stress and predicted shear stress using the relationship provided by Eq. 2. For predicted τ_0 the Darcy friction factor (later converted to C_f using Equation 3) for turbulent motion was approximated using a modified version of the Swamee and Jain (1976) explicit equation:

$$f = \frac{0.25}{\left[\log\left(\frac{k_s}{3.7D_h} + \frac{5.74}{\mathrm{Re}^{0.9}}\right)\right]^2} \tag{4}$$

Where k_s is the roughness height, D_h is the hydraulic diameter, and Re is the Reynolds number ($Re = \rho U_x h/\mu$). Re was calculated for each time step using the average depth measured across the shear plate. U_x at the plate was obtained using the ANUGA inundation model. Equation 4 is based on steady pipe flow experiments and was originally presented with pipe diameter D in the place of the hydraulic diameter D_h. By replacing D with D_h the Darcy friction factor f (and subsequently C_f) may be calculated for each time step.

Using a temporally varying f based on Eq. 4 and the ANUGA model U_x velocity a shear stress may be calculated following Eq. 2. Figure 6 shows the temporal variation of h, U_x, and τ_0 at the dam tip region for an initially dry horizontal bed. The initial peak in measured shear stress shown by the crosses in Fig. 6c is approximately double the calculated. The shear stress continues to be under predicted until $t \approx 2$ s. This implies that it may be inappropriate to calculate shear stress based on conventional steady flow friction factors close to the dam tip. If the analogy between dam break flow and swash uprush exists, Fig. 6c also suggests sediment loads under swash need to be determined using a variable f.

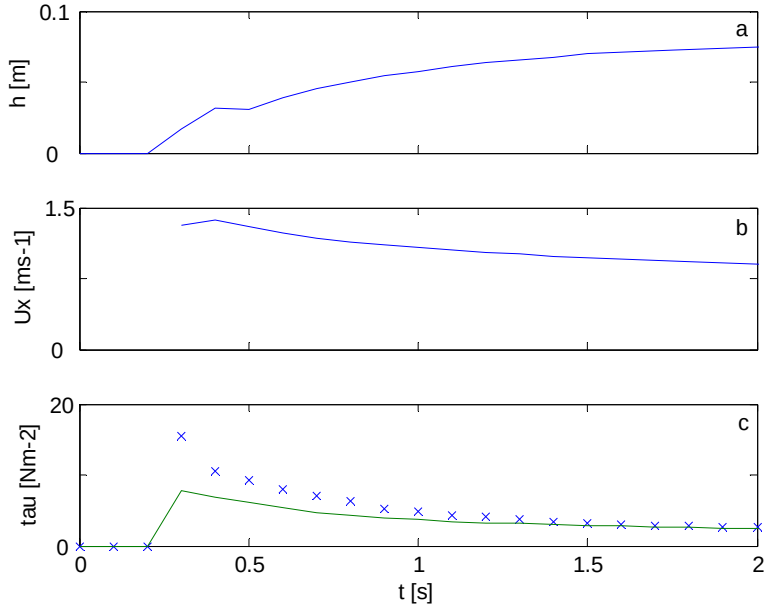

Figure 6. Dam break fluid tip measurements on a horizontal dry bed. (a) h, (b) ANUGA U_x, and (c) τ_0 as a function of time. For (c) "×" measured τ_0, solid line calculated τ_0 using Eq.2.

Wave Flume Experiments

The typical temporal variation of H, U_x (offshore), η, and τ_0 on a 1:10 beach slope close to the SWL and within the lower swash is shown in Figure 7 and 8 respectively. For Fig. 8, the measurement location is $x = 0.27$ m above the SWL and the uprush, or runup, height $R \approx 2.2$ m. For both trials the piston wave maker stroke length $L = 1.4$ m. The similar time series for H and U_x between the two trials is indicative of good experimental repeatability. Surface elevation measurements η obtained via pressure transducers either side of the shear plate indicate a landward directed pressure gradient in the SWL region during bore collapse (Fig. 7). In contrast, no predominant pressure gradient was measured at or behind the uprush tip within the lower swash region (Fig. 8). Shear stress τ_0 time series measurements show a large landward directed spike followed by a rapid decay. At the shear plate, flow reversal occurs at $\tau_0 \approx 0$. For the remainder of the swash cycle (backwash phase) τ_0 is seaward directed. The seaward directed τ_0 is of smaller magnitude and longer duration compared with the landward directed peak. Maximum landward τ_0 was measured in the lower swash. This is consistent with Cox *et al*. (2000) who observed maximum τ_0 to increase between the SWL and the lower swash region. The large, landward directed shear stress of short duration may be a significant contributor to the observed bias in landward sediment transport efficiency on beaches.

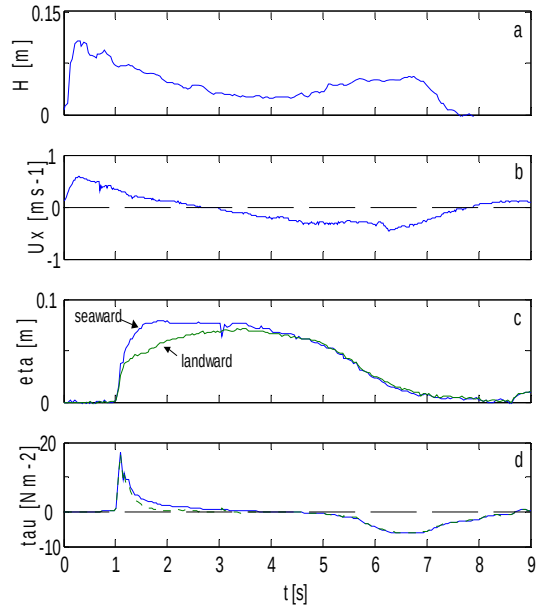

Figure 7. Measurements at SWL on a 1:10 slope beach. (a) offshore bore H, (b) offshore U_x,(c) η at leading and trailing edges of shear plate, and (d) τ_0 as a function of time.

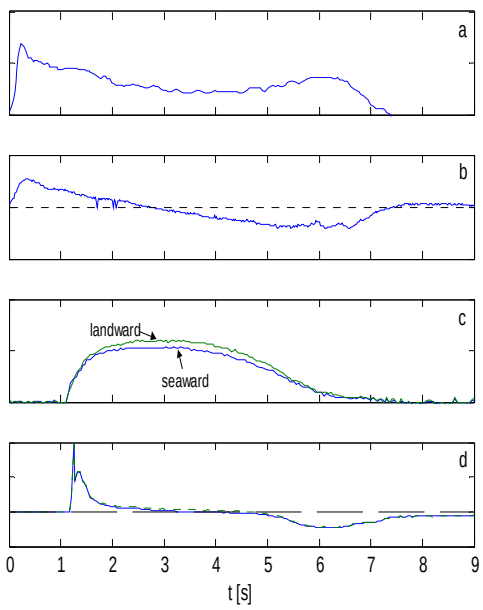

Figure 8. Measurements in lower swash on a 1:10 slope beach. (a) offshore bore H, (b) offshore U_x,(c) η at leading and trailing edges of shear plate, and (d) τ_0 as a function of time.

The pressure measurements taken at the seaward and landward edges of the shear plate suggest a pressure gradient existing across the plate at certain periods during the swash cycle. Considering the relationship between pressure gradient and fluid acceleration, Euler's equation yields for depth averaged horizontal flow (e.g. Dean and Dalrymple, 1991)

$$\frac{DU}{Dt} = \left(\frac{\partial U}{\partial t} + U \frac{\partial U}{\partial x} \right) = -\frac{1}{\rho} \frac{\partial p}{\partial x} = -g \frac{\partial \eta}{\partial x} \tag{5}$$

where DU/Dt is the total acceleration (the local acceleration, $\partial U/\partial t$, plus the convective acceleration, $U\partial U/\partial x$), $\partial p/\partial x$ is the pressure gradient, g is the acceleration due to gravity, and $\partial \eta/\partial x$ is the fluid surface elevation with respect to an arbitrary horizontal datum (refer Baldock *et al*. 2006). Considering Equation 5 with x positive landward, a positive pressure gradient corresponds to a seaward dipping water surface slope and therefore negative total acceleration. A negative pressure gradient corresponds to a landward dipping water surface slope and therefore a positive total acceleration. Fig. 7c shows in the region of the SWL a landward dipping surface exists for $t \approx 1 - 3$ s. For this short period of bore collapse and subsequent uprush directed flow, the landward dipping surface slope will lead to a favourable pressure gradient and perhaps an enhancement of the shear stress. Fig. 8c shows in the lower swash region a seaward dipping surface slope exists for approximately $t \approx 1.5 - 5$ s. During this uprush period, the seaward dipping surface slope will lead to an adverse pressure gradient and perhaps a reduction of the shear stress. Fig. 7c and 8c indicate virtually no pressure gradient during the majority of the backwash phase in the SWL and lower swash region. Further work is required to better understand the implications of pressure gradients on the developing swash boundary layer.

The pressure gradient across the shear plate that may influence the plate's displacement is considered here. Fig. 7c and 7d show a landward dipping surface slope existing for a short

period immediately following the peak in measured shear stress. The corrected shear stress given by the dashed line in Fig. 7d corresponds to the measured shear stress with the secondary pressure forcing removed. In the region at the SWL where the secondary forces are significant the measured shear stress is reduced suggesting a more rapid decay following the initial peak. Fig. 8c and 8d show a seaward dipping surface slope behind the fluid tip for the duration of the uprush phase. The corrected shear stress given by the dashed line in Fig. 8d suggests the presence of an adverse pressure gradient during the swash uprush causes the shear stress measurement to be slightly hindered. The effect of this pressure gradient on plate displacement is considered negligible.

CONCLUSIONS

Conclusions drawn from this paper are based on the preliminary analysis of direct shear stress measurements using a novel shear plate in laboratory scale dam break and solitary wave flumes. For a smooth, impermeable, horizontal bed, comparison between measured and calculated shear stress suggest the shear stress is not well predicted by conventional steady flow theory in the dam break fluid tip (analogous to the swash uprush tip). The peak measured stress at the fluid tip is approximately twice the predicted using steady flow friction factors evaluated at corresponding Reynolds numbers and relative roughness. This large landward directed peak of short duration may be a significant contributor to the observed bias in uprush sediment transport efficiency

The high shear stress at the fluid tip is most likely a result of a very thin boundary layer which has insufficient time to develop as the bed is first wetted. Further work is required to model this process. For the internal flow region the flow history should be considered. Reynolds numbers and relative roughness may be more appropriately defined in terms of the integrated products of velocity and displacement, following the flow, and relative roughness with respect to the boundary layer thickness, δ, as opposed to the depth. Future work will examine this issue.

REFERENCES

Baldock, T. E., and Hughes, M. G. (2005) Field observations of instantaneous water slopes and horizontal pressure gradients in the swash-zone, *Continental Shelf Research*, Vol. 26, No. 5, pp. 574-588.

Butt, T., Russell, P., and Turner, I. (2001) The influence of swash infiltration–exfiltration on beach face sediment transport: onshore or offshore?, *Coastal Engineering*, Vol. 42, pp. 35–52.

Carrier, G. F., Wu, T. T., and Yeh, H. (2003) Tsunami run-up and draw-down on a plane beach, *Journal of Fluid Mechanics*, Vol 475, pp. 79-99.

Conley, D. C. and Griffin, J. G. (2004) Direct measurements of bed stress under swash in the field, *Journal of Geophysical Research (Oceans)*, Vol. 109, p. C03050.

Cowen, E. A., Sou, I. M., Liu, P. L. -F., and Raubenheimer, B. (2003) Particle Image Velocimetry Measurements within a Laboratory-Generated Swash Zone, *Journal of Engineering Mechanics*, Vol. 129, No. 10, pp. 1119-1129.

Cox, D.T., Hobensack, W.A., and Sukumaran, A. (2000) Bottom stress in the inner surf and swash zone, *Proceedings 27th International Conference on Coastal Engineering*, ASCE, pp. 108–119.

Dean, R. G., and Dalrymple, R. A. (1991) Water Wave Mechanics for Engineers and Scientists, World Scientific, Singapore, 353 pp.

Dressler, R. F. (1954) Comparison of Theories and Experiments for the Hydraulic Dam-Break

Wave, *Proceedings of International Association of Scientific Hydrology Assemblée Générale*, Rome, Italy, Vol. 3, No. 38, pp. 319-328.
GE Druck (2006) Automotive Pressure Transducers – PMP 317, website: http://www.gesensing.com/products/pmp_317.htm?bc=bc_ps+bc_drucks.
Grass, A. J., Simons, R. R., Maciver, R. D., Mansour-Tehrani, M., and Kalopedis, A. (1995) Shear cell for direct measurement of fluctuating bed shear stress vector in combined wave/current flow, Proceedings *of XXVIth IAHR Congress: Hydraulic Research and its Applications next Century - HYDRA 2000*, Vol. 1, pp. 415-420.
Gust, G. and Southard, J. B. (1983) Effects of Weak Bed Load on the Universal Law of the Wall, *Journal of Geophysical Research*, Vol. 88, C10, pp. 5939–5952.
Hughes, M. G. (1995) Friction factors for wave uprush, *Journal of Coastal Research*, Vol. 11, pp. 1089-1098.
Jackson, N. L., Masselink, G., and Nordstrom, K. F. (2004) The role of bore collapse and local shear stresses on the spatial distribution of sediment load in the uprush of an intermediate-state beach, *Marine Geology*, Vol. 203, pp. 109–118.
Masselink, G. and Hughes, M. (1998) Field investigation of sediment transport in the swash zone, *Continental Shelf Research*, Vol. 18, pp. 1179-1199.
Masselink, G., Evans, D., Hughes, M. G., Russell, P., (2005) Suspended sediment transport in the swash zone of a dissipative beach, *Marine Geology*, Vol. 216, pp. 169–189.
Microsonic (2005) Instruction Manual, Microsonic GmbH, Dortmund, Germany.
Paola, C. (1986) Skin friction behind isolated hemispheres and the formation of obstacle marks, *Sedimentology*, Vol. 33, pp. 279-293.
Nielsen, O., Roberts, S., Gray, D., McPherson, A., and Hitchman, A. (2005) Hydrodynamic modelling of coastal inundation, *Proceedings of ModSIM 2005*, Melbourne, Australia.
Peregrine, D. H. and Williams, S. M. (2001) Swash overtopping a truncated plane beach, *Journal of Fluid Mechanics*, Vol. 440, pp. 391-399.
Pritchard, D. and Hogg, A.J. (2005) On the transport of suspended sediment by a swash event on a plane beach, *Coastal Engineering*, Vol. 52, pp. 1-23.
Puleo, J. A. and Holland, K. T. (2001) Estimating swash zone friction coefficients on a sandy beach, *Coastal Engineering*, Vol. 43, pp. 25-40.
Raubenheimer, B., Elgar, S., and Guza, R. T. (2004) Observations of swash zone velocities: A note on friction coefficients, *Journal of Geophysical Research*, Vol. 109, p. C01027.
Riedel, P. H. and Kamphuis, J. W. (1973) A shear plate for use in oscillatory flow, *Journal of Hydraulic Research*, Vol. 11, pp. 137-156.
Shen, M. C. and Meyer, R. E. (1963) Climb of a bore on a beach. Part 3. Runup., *Journal of Fluid Mechanics*, Vol. 16, pp. 113-125.
Schlichting, H. (1979) Boundary Layer Theory, McGraw-Hill, New York, USA, 7th edition.
Sontek (2001) Sontek/YSI ADVField/Hydra Acoustic Doppler Velocimeter (Field) Technical Documentation, Sontek/YSI, San Diego, USA.
Swamee, P. K., and Jain, A. K. (1976) Explicit equations for pipe-flow problems, *Journal of the Hydraulics Division*, ASCE, Vol. 102, No. 5, pp. 657-664.